Moving outside of the borehole: characterizing natural fractures through microseismic monitoring

Sherilyn Williams-Stroud,[1*] Jo Ellen Kilpatrick,[1] Brian Cornette,[1] Leo Eisner[1] and Morris Hall[2] **present a case study to illustrate how microseismic events recorded from hydraulic fracture stimulations compare favourably with a separate formation micro-imaging log in the treatment well, and can provide data on fracture characterization away from the borehole.**

Using surface-based arrays to map the locations of induced microseismic events created by hydraulic fracture stimulations is a powerful tool to determine the extent of fractured rock resulting from the treatment. While the geometry of the event locations can be used to infer fracture geometry, in this study we use additional parameters extracted from induced microseismic events (source mechanisms) to determine the specific fracturing behaviour and compare it with independent observations from an FMI (formation micro-imaging) log in the treatment well. We present results of source mechanism analysis for microseismic events triggered by a fracture stimulation treatment in a horizontal well located in the mid continental USA. The source mechanisms have failure planes that closely mirror the orientations of natural fractures in the FMI log. Our results are consistent with the reactivation of natural fractures during the stimulation treatment, suggesting that natural fracture orientations can be determined in cases where image logs are not available. In addition, we show that the microseismic event source mechanisms allow for fracture characterization away from the wellbore, providing critical constraints for building fractured reservoir models.

Background

Monitoring seismic events induced by completions and production processes is becoming an increasingly popular method for operators trying to obtain better estimates of their reserves and understand how a well will behave in production.

These estimates can be further strengthened if the natural fractures in a reservoir can be successfully characterized; for example, these data can play an important role in modelling fluid transport through a formation. Identifying the presence and orientations of natural fractures can be done by analyzing in-situ data from borehole images through techniques including electrical resistivity, acoustic, radar, and ultrasonic image logging (Wu and Pollard, 2002).

Regardless of the technique used, borehole measurements are usually extrapolated to larger scale properties such as seismic anisotropy or coherence in order to characterize reservoir properties between boreholes (Prioul and Jocker, 2009). However, the chaotic nature of these fractures and their significant spatial variability makes extrapolating wellbore measurements of fractures (which are on the centimetre scale) to fractures in the reservoir with a length scale of hundreds of metres extremely challenging.

The study of microseismic events – the low-energy seismic activity emanating from stress-perturbed reservoirs – has long been used in the mining industry as an aid to predict rock burst failure and is increasingly showing promise as a means of characterizing reservoir fractures when borehole image logs are not available. The ability to fully characterize fractures in the reservoir is enhanced by the addition of source mechanism inversions of the microseismic events.

Once relegated solely to the study of seismology, microseismic events have shown a clear link to hydrocarbon producing activities such as hydraulic fracturing, water injection, or fluid production. Mapping these sudden stress changes yields valuable information unavailable from other technology. For example, Rutledge and Phillips (2003) proposed that the orientation of natural fractures controls orientations of failure planes of induced microseismic events, such as those created during reservoir stimulation activities. In their model, small-scale natural fractures coalesce to form larger faults of several metres in length. They observed strike-slip source mechanisms on vertical failure planes for induced microseismic events striking nearly parallel to natural fractures in Cotton Valley rocks (Dutton et al., 1991).

However, Rutledge and Phillips' observations were limited by some of the common restrictions of downhole microseismic monitoring, which include inversion of the signal from a small number of geophones in a limited number of monitoring boreholes (two boreholes in the case

[1] *Microseismic, 1300 W Sam Houston Parkway S, Suite 200, Houston, TX 77042, USA.*
[2] *The Williams Companies, One Williams Center,Tulsa, OK 74172, USA.*
[*] *Corresponding author, E-mail: swmsstroud@microseismic.com*

of the Rutledge and Phillips study) and a bias in the signal that grows as the distance between the geophones and the microseismic event increases. As a result, they were able to determine only a composite (average) focal mechanism from many events grouped on the assumption of mechanism similarity, raising doubts about the accuracy of the observed results (e.g. Šilený et al., 2009).

Microseismic has developed a surface-based measurement system that circumvents some of the challenges of downhole microseismic measurements. The technique utilizes either a dense array of approximately 1000 proprietary surface geophones, or a less dense array of geophones buried a few hundred feet in the shallow subsurface to detect and locate microseismic energy emissions.

It is true that compared to downhole arrays in a nearby well, the greater distance between the receivers and the events for surface arrays results in a lower signal-to-noise ratio for each individual receiver. However, the 1000-fold stacking of the signal from many surface receivers enhances the signal and additionally, because all of the surface geophones are nearly the same distance from the event, there is no systematic bias of the inversion due to location.

Case study

Surface-based microseismic monitoring was carried out to assess the effectiveness of two different fluids used for fracture stimulations in a horizontal well with a 1070 m lateral drilled in the Arkoma Basin of Oklahoma. Slick-water was used to treat the well from the toe to mid lateral, while nitrogen was used to treat the well from mid lateral to the heel.

The monitoring array consisted of 1078 stations of 12 geophones, laid out in a radial pattern around the treatment well (Figure 1). The geophones were buried to a depth of approximately 30 cm to maximize the signal-to-noise ratio by reducing the interference of the frequent seasonal rainfall. The surface array design and subsequent seismic processing also factored in cultural sources of noise, such as traffic and inherent pad noises. A total of 25 hours of data were recorded and processed.

Microseismic events induced by the hydraulic fracturing were detected by the geophones in the surface array and then located by a beamforming process known as passive seismic emission tomography (PSET), which is essentially a one-way depth migration. A layered velocity model was calculated using the perforation shots from each treatment as sources for calibration events. By taking a measurement of the arrival times across the array and plotting them against the distance between receivers, a velocity estimate from the well depth to the surface was derived. Receiver statics were calculated from the perforation shot arrivals and used to complete the calibration of the model.

Two important points were observed that gave high confidence in good velocity calibration. Firstly, the derived velocities were highly consistent with root mean square velocities calculated from a sonic log that was taken on the treatment well bore. Secondly, using the calibrated model,

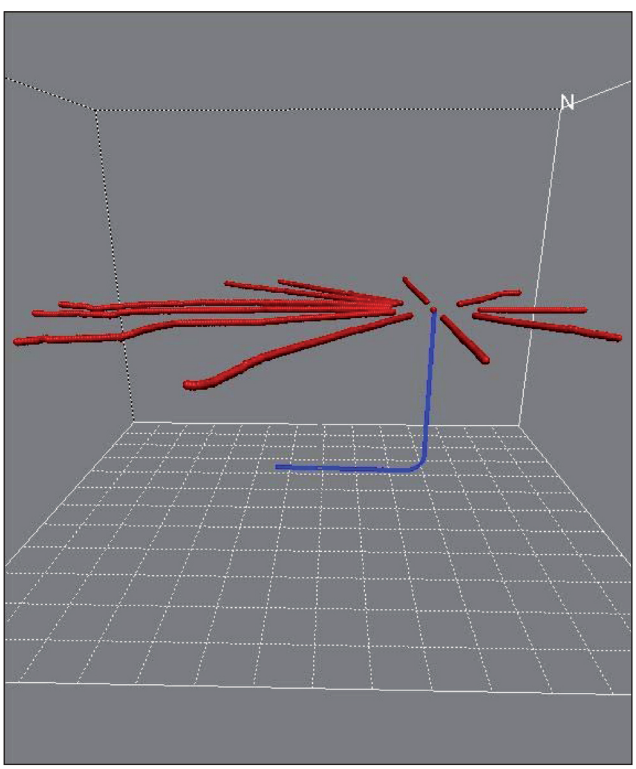

Figure 1 *Monitoring array geometry (red symbols) relative to well (in blue), depth of the 1070 m lateral is about 1200 m. View is looking west.*

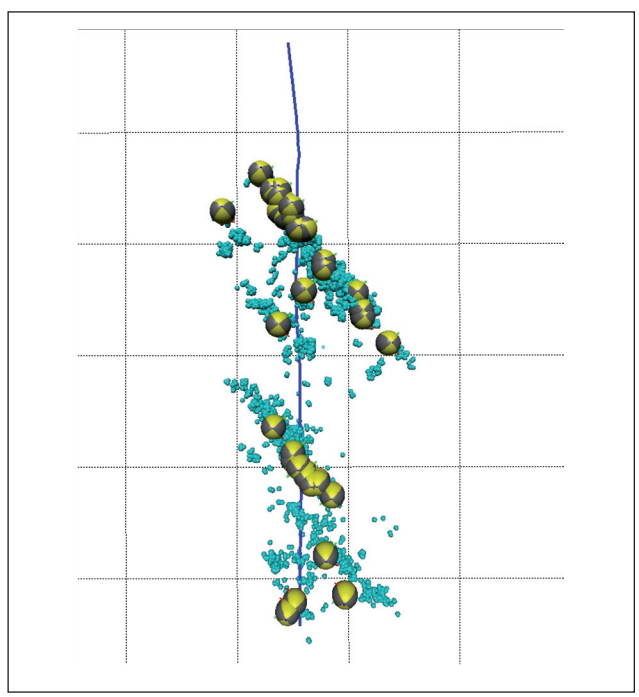

Figure 2 *Map view of microseismic events showing locations of source mechanisms. The cyan dots show all microseismic events that were detected and located. On the beach balls representing the source mechanisms, the yellow quadrants represent compression and the gray areas represent tension. Grid line interval is 500 ft (152 m).*

the events corresponding to the perforation shots located to within 15 m of their measured location in the well bore.

The observed locations of microseismic events induced by the stimulation treatments suggested that planar fractures were created with varying complexity (Figure 2). We detected thousands of events at the reservoir level; from those we selected 44 of the most representative and with the highest signal-to-noise ratios, and inverted them for their source mechanisms (Hall and Kilpatrick, 2009).

Source mechanism inversion

We performed source mechanism inversion on the surface data based on a least squares inversion of the observed compression (P-wave) amplitudes recorded on the vertical components of recording geophones. Knowing the source mechanism of the events not only allows us to improve the location accuracy of the events, it also provides information to build a reservoir model that is consistent with what the measured data was telling us. The inversion algorithm uses the same data to obtain the full moment inversion (including the volumetric part of the source mechanism), and the double-couple (shear) mechanism solutions, allowing us to determine source mechanism without restrictions imposed by observation geometry. In both cases, a point source was assumed. The moment tensor representing the source mechanism was inverted from a point source relationship between observed displacements on a vertical component and moment tensor components.

It is possible to use multiple waves observed at the surface (such as P- and S-waves) for inversion of the moment tensor, but only amplitudes of direct P-waves on vertical receiver components were used in this study because they provided a robust inversion result independent of the poorly constrained S-wave velocity model. We used the Green's function derivatives in which we assumed a homogeneous isotropic medium in the inversion, with correction for free surface and attenuation. Although there was inherent heterogeneity of the velocities and densities that could impact the source mechanism inversion, the broad distribution of the surface receivers over multiple offsets and azimuths compensated for model heterogeneity and provided accurate estimates of fault plane orientations, as observed by others (Šilený, 2009). The fact that we obtained such a good fit between the observed and modelled P-wave amplitudes (as shown in Figure 3) further verified this compensation effect.

This dataset demonstrated microseismic events with both pure shear and more complex mechanisms. The more complex mechanisms have a significant non-double couple component which can be characterized as tensile opening along nearly vertical fault planes with orientation very close to the events with pure shear mechanisms. Analysis of the particle motion of P-waves due to full mechanism inverted from the surface monitoring array is shown in Figure 4. For

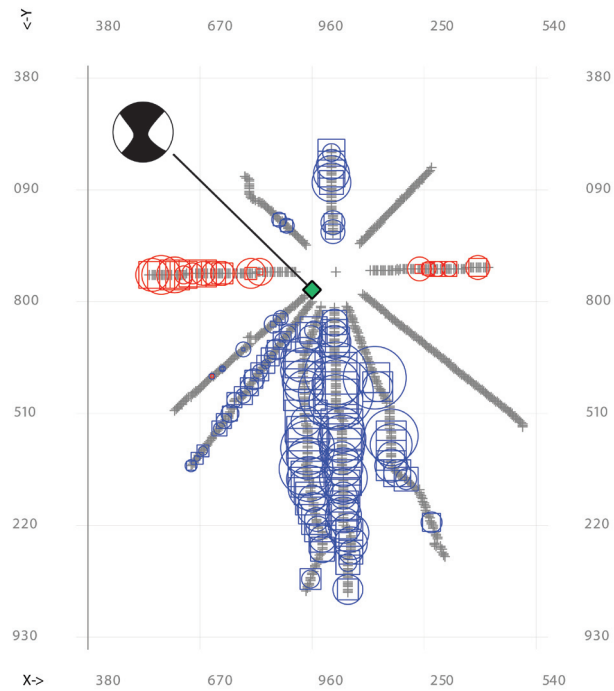

Figure 3 *Source mechanism represented by a lower hemisphere projection (top right) and its fit to the observed P-wave amplitudes for a typical microseismic event in this dataset. Blue and red circles represent up and down first motion of the direct P-waves. Squares analogously represent synthetic amplitudes of direct P-waves.*

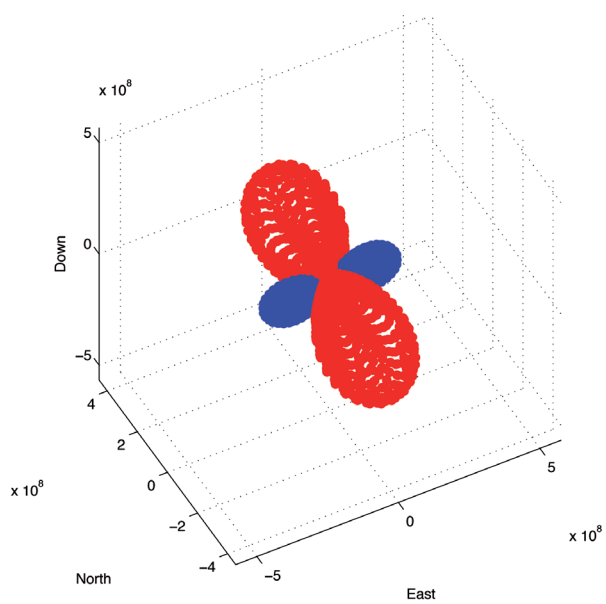

Figure 4 *3D view of P-wave particle motion of inverted source mechanism from Figure 2. The red colour represents outward motion, the blue colour represents inward motion, and the distance from the centre of the plot is proportional to the P-wave amplitude. (Units in Nm)*

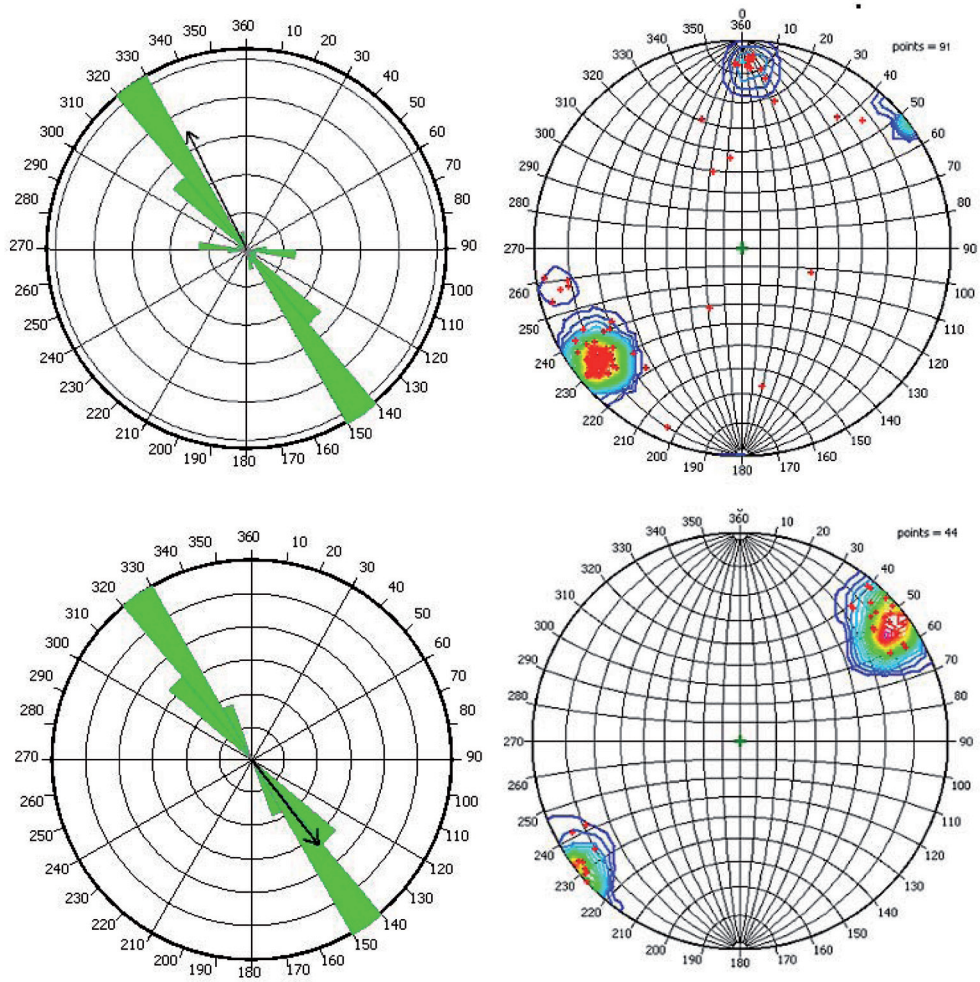

Figure 5 *Orientations of natural fractures interpreted from an image log (top row) and calculated from the source mechanism inversion (bottom row).*

a pure shear source, both inward and outward lobes would be symmetrical, however the inverted figure shows asymmetry with a larger opening component. This component can be explained by approximately north-south opening and represents less than 10% of the total moment. The broad azimuthal and offset coverage afforded by the monitoring array allowed for generalized inversion of both shear and non-shear mechanisms. This further allowed us to reliably determine dips and strikes of the inverted fault planes, even in the case of significant tensile components of the source mechanisms (Šílený, 2009).

A number of tests were performed to investigate the stability of the inverted results. These included randomly removing approximately 10% of the receivers and repeating inversion for source mechanisms, and also testing the inversion by picking opposite arrivals on receivers with weak signal-to-noise ratio. These tests resulted in only minor changes to the inverted mechanism, and variability of the inverted dips and strikes was at most 3–4°. Therefore, we conclude that the inverted variations (5–10°) in strikes and dips of the fault planes represent true variation in source mechanism orientations.

The inverted mechanism of the representative events in Figure 2 is very close to a pure strike-slip mechanism, as 90% of the inverted moment is due to pure shear motion along nearly vertical fault planes (dip 89° and 81°). Our results show that this mechanism provided ample energy to be accurately located, and that the assertion by Chambers et al. (2010) that strike-slip events are very difficult to locate from surface geophone arrays is incorrect. The accuracy of the location was further verified by moving the seismic traces out with calculated travel-time delays, which flattened within 15 ms across the entire array. The corresponding seismic moment of the event shown in Figure 3 was approximately 3.4 10^7 Nm, corresponding to magnitude -1.1.

Fracture analysis

The FMI log acquired in the same well identified natural fractures, with the natural fracture orientation maximum

at 84°/46° dip/dip azimuth. The source mechanism solution planes from the induced microseismicity compliment the FMI log, showing nearly identical orientations to the natural fractures measured in the wellbore and indicating that the existing natural fractures were reactivated during the treatment (Figure 5).

The source mechanisms indicate strike-slip reactivation of existing fractures. A non-shear component of the inverted mechanisms is also present, indicating opening-mode failure mechanisms are also active, providing space where fracturing fluids and proppants could invade fault planes. Fractures interpreted in the image log include open and partially open natural fractures, as well as drilling-induced fractures with orientations that could be influenced by the existence of natural fractures. The in-situ stress indicators in the image log are primarily en-echelon tensile fractures oriented nearly east-west, but a few north-south breakouts are also identified. Observations of both types of borehole stress indicators (breakout and tensile fractures) have been reported in other wells where the tectonic stress regime is strike-slip (Barton et al., 1998). The maximum horizontal stress direction of 88° azimuth from the drilling induced fractures is consistent with the stress directions inferred from the T- and P- axes of the source mechanism inversion solutions, so that the same conclusion can be derived via either method.

By characterizing fractures and determining their locations and orientations through fault planes inverted from microseismic events, we obtain a higher-resolution characterization away from the wellbore. The combination of source mechanisms and event locations allows us to populate a geocellular model with fractures away from the wellbore.

For those events that were below the signal-to-noise threshold necessary for source mechanism inversion, we applied a stochastic approach to generating fractures, which also allowed for exploration of the larger location uncertainty associated with smaller events. Figure 6 shows one realization of a DFN (discrete fracture network) model generated using this two-part approach. The wellbore image log analysis of the natural fracture orientations includes a secondary orientation maximum of steeply-dipping conductive natural fractures with a strike about 10° from the drilling induced fractures (shown in Figure 5). These fractures are also oriented within the in-situ stress field so that they have a high slip tendency, but will have a larger tensile component than the NW-SE oriented natural fractures.

Including the secondary fracture set in the DFN may provide the enhanced permeability required to achieve a history match using fracture flow properties calculated from the DFN. Although these fracture orientations are not resolved by source mechanism inversion, the knowledge of the geomechanical behaviour of the reservoir obtained from the image log and the confirmation of reactivation of natural fractures from the inverted source mechanisms allows us to infer their mutual stimulation in areas of microseismicity.

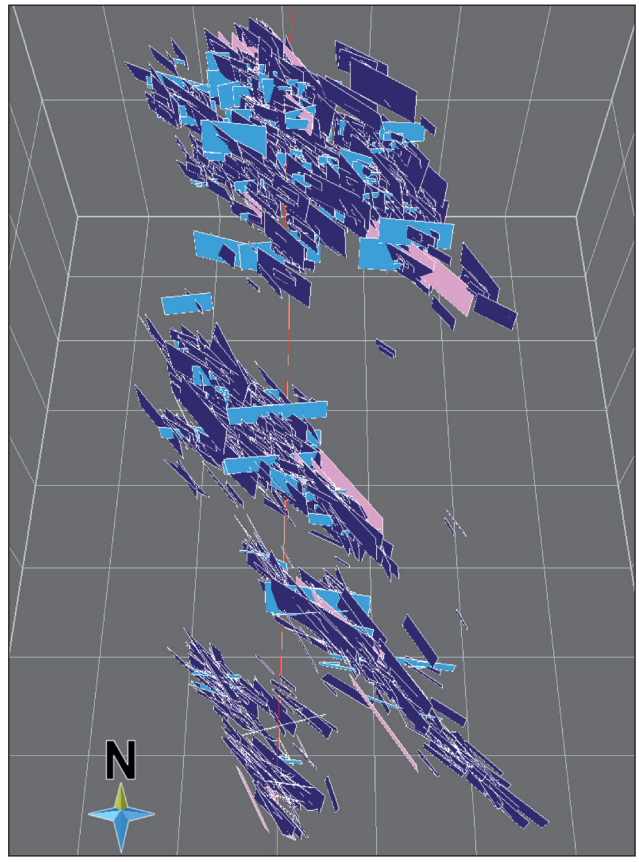

Figure 6 *DFN model of fractures based on microseismic events. The fracture orientations are based on the statistics of the natural fractures interpreted from the FMI log. Fractures coloured cyan represent the secondary more E-W fracture orientation. The deterministic fractures, i.e. fractures explicitly included at the location of a source mechanism inversion are coloured pink.*

The result is a highly constrained upscaling of properties measured from the wellbore at a small scale and populated to the reservoir volume away from the well, a unique finding that demonstrates a new application for microseismic measurements.

Conclusions

This study provided a unique opportunity to examine how microseismic events induced by hydraulic fracturing and measured by a large surface-based array compare with results obtained by FMI on the same well. We found remarkable agreement with the fault planes of individual microseismic events demonstrating similar strikes and dips as natural fractures observed in the FMI log. This observation provides insight into both the physics of the induced seismic events (i.e., reactivation of natural fractures) and the possibility of natural fracture characterization away from the wellbore, an analysis that was previously reserved to the domain of seismic anisotropy.

This characterization is used to create a DFN of the reservoir rock based on deterministic fractures where locations and orientations are explicitly resolved and on stochastic fractures where events are detected, but their mechanisms are not determined. The result is a reservoir property distribution based on the events that bridge the scales between reservoir and borehole data.

In addition, the close agreement between microseismic and FMI measurements indicates that, for the first time, it is possible to characterize the fractures within a reservoir using only microseismic data. This is an important development, particularly for those wells in which borehole image logs are not available.

Acknowledgements

The authors thank Williams Company for release of this dataset for publication.

References:

Barton, C.A., Castillo, D. A., Moos, D., Peska, P. and Zoback, M.D. [1998] Characterizing the full stress tensor based on observations of drilling-induced wellbore failures in vertical and inclined boreholes leading to improved wellbore stability and permeability prediction. *APPEA Journal 1998*, 29-53.

Chambers, K., Kendall, J-M. and Barkved, O. [2010] Investigation of induced microseismicity at Valhall using the Life of Field Seismic array. *The Leading Edge*, **29**(3), 290-295.

Dutton, S. P., Laubach, S. E., Tye, R. S. and Diggs, T. N. [1991] Geological analysis of the Travis Peak formation and Cotton Valley sandstone. *Gas Research Institute Report GRI-91/0048*.

Hall M. and Kilpatrick, J. [2009] Surface microseismic monitoring of slick-water and nitrogen fracture stimulations, Arkoma Basin, Oklahoma. *79th SEG Annual Meeting, Expanded Abstracts*, 28(1), 1562-1565.

Prioul R. and Jocker J. [2009] Fracture characterization at multiple scales using borehole images, sonic logs, and walkaround vertical seismic profile. *AAPG Bulletin*, **93**, 1503-1516.

Rutledge, J.T. and Phillips, W.S. [2003] Hydraulic stimulation of natural fractures as revealed by induced microearthquakes, Carthage Cotton Valley gas field, east Texas. *Geophysics*, **68**, 441–452.

Šílený, J., Hill, D. P., Eisner, L. and Cornet, F. H. [2009] Non-double-couple mechanisms of microearthquakes induced by hydraulic fracturing. *J. Geophys. Res.*, **114**, B08307.

Šílený, J. [2009] Resolution of non-double-couple mechanisms: simulation of hypocenter mislocation and velocity structure mismodeling. *Bull. Seis. Soc. of A.*, **99**, 2265-2272.

Wu, H. and Pollard, D. D. [2002] Imaging 3-D fracture networks around boreholes. *AAPG Bulletin*, **86**(4), 593-604.